Dermatol Ther (Heidelb) (2025) 15:2495–2520
https://doi.org/10.1007/s13555-025-01454-7

ORIGINAL RESEARCH

Translational Pharmacokinetics of Icotrokinra, a Targeted Oral Peptide that Selectively Blocks Interleukin-23 Receptor and Inhibits Signaling

Beverly Knight · Brinda Tammara · Nishit B. Modi · Shannon Dallas · Saro Mardirosian · Jianyao Wang · Aline Laenen · Laurent Leclercq · Karen DiLoreto · Lieve Adriaenssen · Darren Moss · David Polidori · Siladitya Ray Chaudhuri · Seonghee Park · Carlo Sensenhauser · Anthony Ndifor · Siddharth Sukumaran · Tristan Baguet · Yifan Shi · Shefali Patel · Brian Geist · Anne Fourie · Raymond Patch · Chengzao Sun · Stephanie A. Barros · Sandeep Somani · Mario Monshouwer

Received: April 11, 2025 / Accepted: May 22, 2025 / Published online: July 8, 2025

ABSTRACT

Introduction: Icotrokinra (formerly JNJ-77242113 or PN-21235) is a targeted oral peptide that selectively inhibits interleukin-23 receptor signaling. The studies described here assessed its absorption, distribution, metabolism, and excretion (ADME), and potential for drug–drug interactions (DDI).

Methods: In vitro assays evaluated permeability, plasma protein binding, blood-to-plasma partitioning, metabolic stability, and interactions with drug transporters and metabolic enzymes. The nonclinical pharmacokinetic properties of icotrokinra were studied in vivo in rats and monkeys. Phase 1 studies evaluated the pharmacokinetic profile, metabolic profile and excretion in healthy volunteers.

Former Johnson & Johnson Employee: Anne Fourie, Raymond Patch, Chengzao Sun, Sandeep Somani.

Prior Publication: Limited data have been previously published in Fourie AM, Cheng X, Chang L, Greving C, Li X, Knight B, Polidori D, Patrick A, Bains T, Steele R, Allen SJ, Patch RJ, Sun C, Somani S, Bhandari A, Liu D, Huie K, Li S, Rodriguez MA, Xue X, Kannan A, Kosoglou T, Sherlock JP, Towne J, Holland MC, Modi NB. JNJ-77242113, a highly potent, selective peptide targeting the IL-23 receptor, provides robust IL-23 pathway inhibition upon oral dosing in rats and humans. Sci Rep. 2024;14(1):17515.

Prior Presentation: Limited data have been previously presented as a poster at the ASCPT 2025 Annual Meeting, 28–30 May in Washington, D.C., USA in B. Knight, S. Dallas, S. Mardirosian, J. Wang, A. Laenen, L. Leclercq, D. Moss, K. DiLoreto, S. Park, D. Polidori, C. Sensenhauser, A. Ndifor, Y. Shi, S. Patel, A. Fourie, R. Patch, C. Sun, M. Monshouwer. PII-056 ADME profiling of targeted oral peptide JNJ-77242113.

Supplementary Information The online version contains supplementary material available at https://doi.org/10.1007/s13555-025-01454-7.

B. Knight (✉) · D. Polidori · S. R. Chaudhuri · A. Ndifor · A. Fourie
Johnson & Johnson, San Diego, CA, USA
e-mail: bknight3@its.jnj.com

B. Tammara · S. Dallas · S. Mardirosian · J. Wang · K. DiLoreto · S. Park · C. Sensenhauser · S. Sukumaran · Y. Shi · S. Patel · B. Geist · R. Patch · C. Sun · S. A. Barros · S. Somani
Johnson & Johnson, Spring House, PA, USA

N. B. Modi
Protagonist Therapeutics, Inc, Newark, CA, USA

A. Laenen · L. Leclercq · L. Adriaenssen · D. Moss · T. Baguet · M. Monshouwer
Johnson & Johnson, Beerse, Belgium

C. Sun · S. Somani
Pinnacle Medicines, Doylestown, PA, USA

***Results*:** Icotrokinra demonstrated oral bioavailability of 0.1–0.3% in animals, with evidence of systemic pharmacodynamic activity, without the use of an absorption enhancer. The compound was stable across species in plasma, gastrointestinal matrices, and hepatocytes. Protein binding was low across species (~ 50% in human plasma), and icotrokinra distributed freely to tissues, including skin, joints, and gastrointestinal tissues. Following oral dosing in both rats and monkeys, fecal excretion of unabsorbed drug was the primary elimination route, and metabolite levels were low (each < 2% of dose) in plasma and excreta, with unchanged icotrokinra being the main circulating component. Icotrokinra was neither a substrate nor an inhibitor of prototypical drug transporters or cytochrome P450 enzymes. Icotrokinra exhibited dose-proportional pharmacokinetics from 25 mg to 1000 mg in a first-in-human study, and no serious adverse events were identified following single and multiple dose administrations. Unchanged icotrokinra was the only drug-related component in human plasma.

***Conclusions*:** Icotrokinra exhibited high stability and an ADME profile consistent with that of a small peptide, with no risk of DDI identified on the basis of in vitro studies. Clinical data demonstrated linear pharmacokinetics and no major metabolites.

***Trial Registration Number*:** ClinicalTrials.gov, NCT04621630. Euclinicaltrials.eu, EUCT: 2023-504720-26-00.

A Graphical Abstract is available for this article.

Graphical abstract:

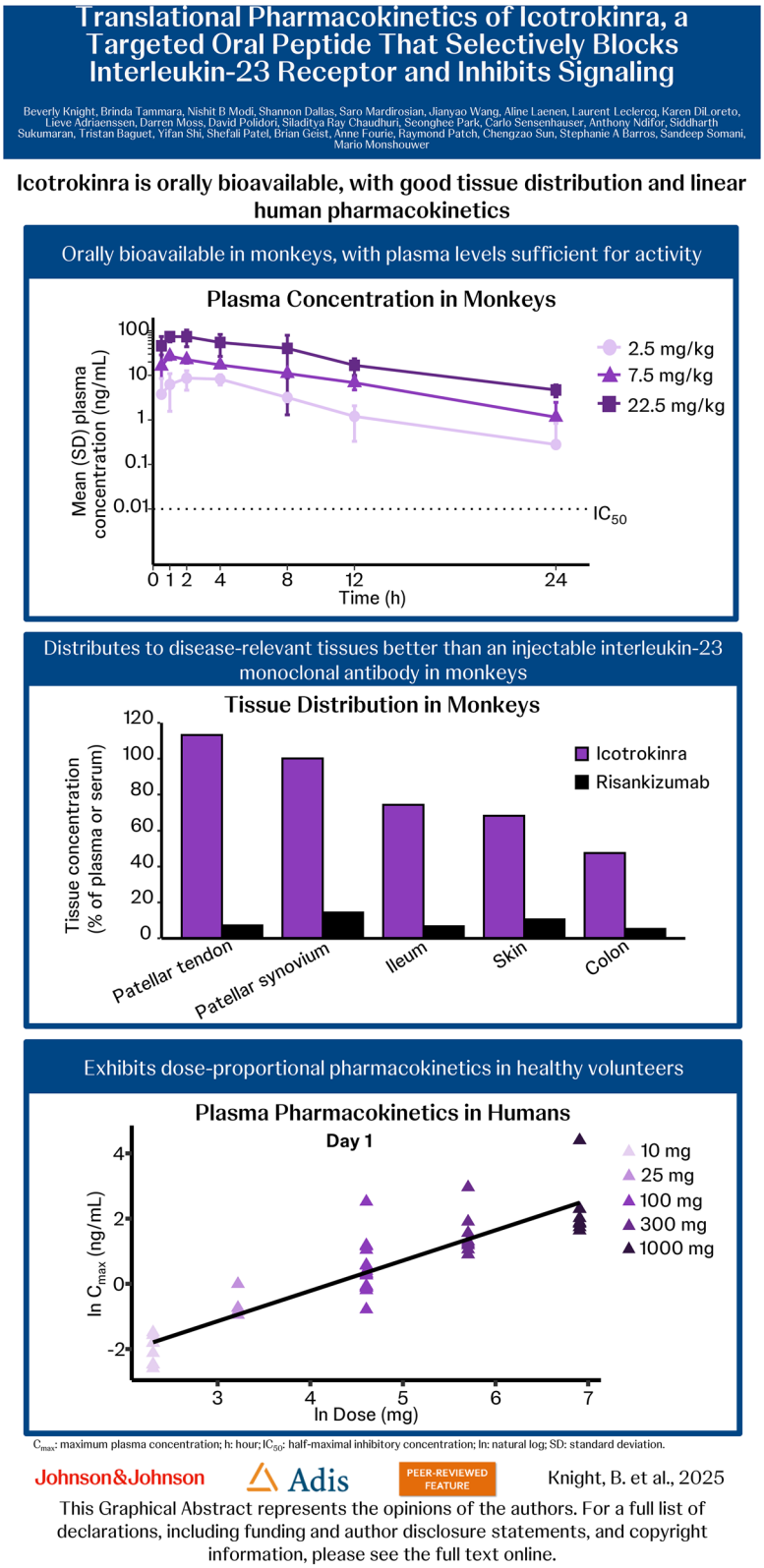

Keywords: ADME; IL-23; Targeted oral peptide; Pharmacokinetics; Psoriasis; Icotrokinra

Key Summary Points
Why carry out this study?
Despite their convenience, approved oral therapies for the treatment of chronic inflammatory diseases have shown lower efficacy and greater safety concerns compared with biologics, highlighting the need for better oral treatment options.
The study evaluated, for the first time, the nonclinical and clinical pharmacokinetic aspects of icotrokinra, a first-in-class, targeted oral peptide that selectively inhibits interleukin (IL)-23 signaling by binding to the IL-23 receptor.
What was learned from the study?
Icotrokinra shows high stability compared with typical peptides, is orally bioavailable, demonstrates systemic pharmacology, and distributes to disease-relevant tissues better than the injectable IL-23 monoclonal antibody, risankizumab.
Icotrokinra exhibits dose-proportional pharmacokinetics with no safety signals identified following oral administration in healthy volunteers
The pharmacokinetic findings for the first-in-class, targeted oral peptide icotrokinra, including its high stability and potency, provide support for further clinical development.

DIGITAL FEATURES

This article is published with digital features, including a graphical abstract, to facilitate understanding of the article. To view digital features for this article, go to https://doi.org/10.6084/m9.figshare.29128130.

INTRODUCTION

Interleukin (IL)-23 and its receptor (IL-23R) play a crucial role in regulating immune responses, particularly within the context of chronic inflammatory and autoimmune diseases including psoriasis, psoriatic arthritis, and inflammatory bowel disease (IBD) [1]. Interaction between IL-23 and IL-23R promotes expansion and survival of T helper (Th)17 cells that secrete IL-17A, IL-17F, IL-22, and other inflammatory mediators [1]. Extensive experimental and clinical data establishing the safety and efficacy of anti-IL-23-therapies has led to the approval of biologics targeting the IL-23p19 subunit, e.g., guselkumab and risankizumab, for the treatment of psoriatic skin and joint disease [2], as well as IBD [3].

Oral delivery of agents for the treatment of chronic inflammatory diseases offers a convenient alternative to injectables [4–6]; however, currently approved oral therapies have exhibited lower efficacy and additional safety concerns compared with biologics [7–9]. Thus, an unmet need remains for novel, improved oral treatments. Despite offering high binding specificity and affinity, poor intestinal stability and permeability have limited the use of biologically active peptides as oral therapies. Recent advances in peptide design, including macrocyclization, have led to improvements in oral absorption and bioavailability [10, 11].

Icotrokinra (formerly JNJ-77242113 or PN-21235) is a macrocyclic peptide (Fig. 1) that selectively inhibits IL-23R [12]. Unlike previously approved therapies targeting the IL-23 pathway, icotrokinra can be administered orally. In animal models of IBD and skin inflammation, orally administered icotrokinra attenuated inflammation in colon and skin tissues, while significantly inhibiting expression of IL-23-induced proinflammatory cytokines (IL-17A, IL-17F, and IL-22) to levels comparable with an injectable anti-IL-23 monoclonal antibody [12]. Icotrokinra also potently and specifically inhibited proximal IL-23-induced signaling and downstream interferon (IFN)γ production in blood from healthy donors and participants with psoriasis [12].

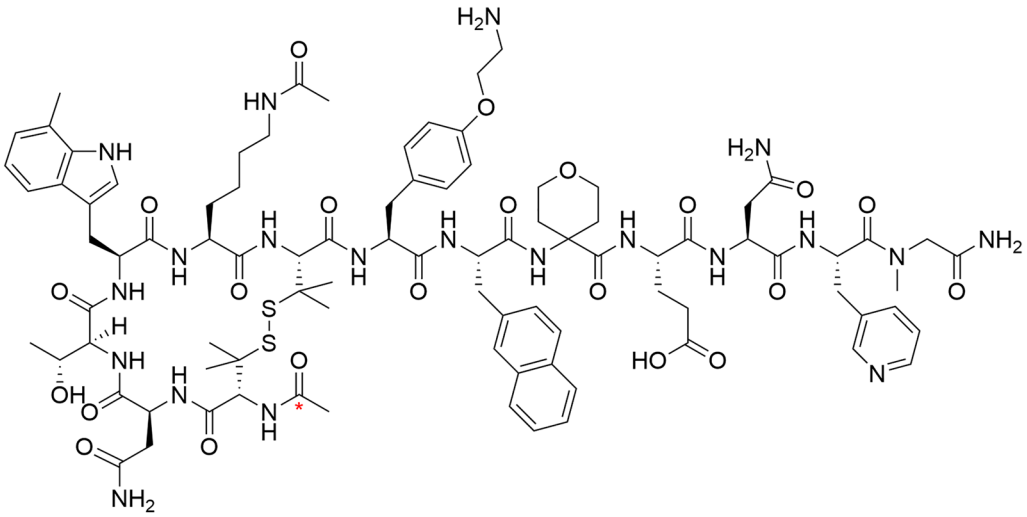

Fig. 1 Chemical structure of icotrokinra. Sequence: Ac-cyclo[Pen-Asn-Thr-7MeTrp-Lys(Ac)-Pen]-Phe(2ae)-2Nal-ThpGly-Glu-Asn-3Pal-Sar-NH2. Asterisk indicates position of [^{14}C] label at the N-terminal acetyl group for [^{14}C]-icotrokinra

In the Phase 2b FRONTIER 1 study (NCT05223868), icotrokinra met its primary endpoint, demonstrating a significant dose–response for achievement of ≥ 75% reduction in the Psoriasis Area and Severity Index (PASI) score (PASI 75) response at week 16 ($P < 0.001$) in participants with moderate-to-severe psoriasis [13]. The highest clinical response rates were generally observed with icotrokinra 100 mg taken once or twice daily, with 79% of participants in the 100 mg twice daily group achieving PASI 75 and 40% attaining complete skin clearance (PASI 100). Through week 16, rates of adverse events (AEs) were similar across the icotrokinra and placebo groups, and no relationship was identified between icotrokinra dose and the incidence of AEs. In the long-term extension FRONTIER 2 study (NCT05364554), icotrokinra demonstrated sustained response rates, with no safety signals identified through 1 year of treatment [14].

The aims of this report were to evaluate the ADME properties of icotrokinra and to assess its potential for DDI to better understand the benefit–risk profile of this therapy. In vitro and in vivo nonclinical studies were conducted to elucidate the ADME properties and DDI potential of icotrokinra, and clinical studies assessed its pharmacokinetic (PK) profile and safety in healthy participants.

METHODS

A brief description of the methods is provided below. Additional details can be found in the supplement.

Icotrokinra comprises 13 amino acids with 12 stereocenters (Fig. 1). The final drug substance used in these studies was > 95% pure with > 95% enantiomeric excess. Ultra-high performance liquid chromatography (UHPLC) was used to identify impurities, including potential epimers.

Nonclinical In Vitro Assays

Permeability and Efflux

Bi-directional permeability of [^{14}C]-icotrokinra was assessed in multidrug resistance protein 1 (MDR1)-transfected Lilly Laboratories cell-porcine kidney (LLC-PK1-MDR1) and

mock-transfected (LLC-PK1-mock) cell monolayers (see Supplementary Methods Sect. 1.1.1).

Protein Binding and Blood-to-Plasma Partitioning

The extent of plasma protein binding of icotrokinra was assessed in vitro in C57BL/6 mouse, Sprague Dawley rat, New Zealand White rabbit, cynomolgus monkey, and human plasma, as well as in human purified plasma proteins albumin and α-1-acid glycoprotein (AAG), using an equilibrium dialysis method (see Supplementary Methods Sects. 1.1.2–1.1.3).

Whole blood (WB) to plasma partitioning ratio ($K_{WB/P}$) and red blood cell (RBC) to plasma partitioning ratio ($K_{RBC/P}$) were determined by incubating icotrokinra with Sprague Dawley rat, beagle dog, cynomolgus monkey, and human whole blood.

Metabolic Stability

The stability of icotrokinra was assessed by incubation with: fecal homogenates from Sprague–Dawley rats, cynomolgus monkeys, and human donors; gastrointestinal (GI) mucosa from pooled Sprague–Dawley rats, pooled cynomolgus monkeys, and single donor humans; and simulated gastric fluid (SGF) and purified GI enzyme matrices including chymotrypsin, pancreatin, pepsin, and trypsin (see Supplementary Methods Sect. 1.1.4).

Drug–Drug Interaction Studies

Studies were performed using transfected cell systems or vesicles to determine whether icotrokinra is a substrate or inhibitor of various transporters using: human embryonic kidney (HEK) 293 mock-transfected (control) cells and organic anion transporter (OAT)P1B1, OATP1B3, OAT1, and organic cation transporter (OCT)2-overexpressing cells; Madin-Darby canine kidney (MDCK)-II parental (control) cells and OAT3, multidrug and toxin extrusion (MATE)1 or MATE2-K overexpressing cells; LLC-PK1 cell line mock-transfected or human breast cancer resistance protein (BCRP) expressing cells; and inside-out membrane vesicles overexpressing human bile salt export pump (BSEP). The ability of icotrokinra to inhibit the major human cytochrome P450 (CYP) isoforms (CYP1A2, 2B6, 2C8, 2C9, 2C19, 2D6, 2E1, and 3A4), as well as the potential mRNA induction of human CYP1A2, CYP2B6, and CYP3A4, were evaluated using cryopreserved human hepatocytes (see Supplementary Methods Sect. 1.1.5).

Nonclinical In Vivo Studies

Nonclinical in vivo PK studies were performed in rats and monkeys. Analytical methods are described in the supplementary material. Noncompartmental PK analyses were done using Phoenix™ WinNonlin® (Certara LP) and were summarized using descriptive statistics.

Plasma PK profiles were determined following single doses of icotrokinra administered by intravenous (IV) injection (2 mg/kg; in 10 mM PBS) or orally (20 mg/kg; 50 mM sodium phosphate buffer; and 30, 100, and 300 mg/kg; 10 mM PBS) to fasted Sprague Dawley rats ($n=3$/group). Blood was collected for up to 24 hours (h) (see Supplementary Methods Sect. 1.2.1).

Plasma PK profiles were determined following a single dose of icotrokinra administered by intravenous (IV) injection (1 mg/kg; in PBS) or orally (2.5, 7.5, and 22.5 mg/kg; in 50 mM sodium phosphate buffer) to fasted cynomolgus monkeys ($n=4$/group). Blood was collected for up to 24 h (see Supplementary Methods Sect. 1.2.2).

A PK study was conducted to determine the tissue distribution of icotrokinra following a 1 mg/kg (in 20% HP-β-CD) IV injection to cynomolgus monkeys ($n=4$) on two consecutive days. Plasma PK was assessed on Day 1. On Day 2, animals were sacrificed and tissue samples were collected at 1.5 and 6 h post-dose ($n=2$/timepoint; see Supplementary Methods Sect. 1.2.3).

The tissue distribution of risankizumab was determined following a 2 mg/kg IV injection to cynomolgus monkeys ($n=4$). On Day 7 post administration, serum and tissue samples were collected ($n=4$/timepoint; see Supplementary Methods Sect. 1.2.4).

Icotrokinra metabolism was investigated following a single dose of [^{14}C]-icotrokinra administered orally (300 mg/kg [~ 400 µCi/kg]; in 50 mM phosphate) to fasted Sprague Dawley rats ($n = 2$). Urine, feces, and blood were collected through 24 h and metabolite profiles were obtained (see Supplementary Methods Sect. 1.2.5).

Icotrokinra excretion was investigated following a single dose of [^{14}C]-icotrokinra administered orally (300 mg/kg [~ 400 µCi/kg]; in 50 mM phosphate) to fed Sprague Dawley rats ($n = 3$). Urine and feces were collected for 96 h (see Supplementary Methods Sect. 1.2.6).

The metabolism and excretion of icotrokinra were investigated following a single dose of [^{14}C]-icotrokinra administered orally (300 mg/kg [~ 100 µCi/kg] in water) to fasted cynomolgus monkeys ($n = 2$). Blood samples were collected from all animals for up to 48 h and urine and feces were collected through 96 h (see Supplementary Methods Sect. 1.2.7).

Phase 1 Studies in Healthy Participants

Study Design

First-in-Human Study This was a single-center, randomized, double-blind, placebo-controlled, single and multiple ascending dose study to assess the safety, tolerability, PK, and pharmacodynamics (PD) of icotrokinra in healthy adult participants. The study was conducted in two parts: the single ascending dose (SAD) and the multiple ascending dose (MAD), with each part involving a different set of participants. SAD was a sequential single dose-escalation design with five cohorts, with participants randomized to receive placebo ($n = 2$) or icotrokinra ($n = 6$). Single icotrokinra doses of 10 mg, 25 mg, 100 mg, 300 mg, or 1000 mg were administered as an oral solution (in 50 mM sodium phosphate, pH 7.4) following an overnight fast. MAD was a sequential multiple dose-escalation design with five cohorts using the same five dose levels as the SAD, and participants randomized into the placebo ($n = 2$) or icotrokinra ($n = 8$) groups. Approximately 22–30 h following their last dose, participants receiving the 25 mg dose underwent sigmoidoscopy to obtain mucosal colon and rectal tissue biopsy samples to measure tissue drug levels. An additional sixth cohort (100 mg) was added and underwent sigmoidoscopy for collection of mucosal tissue samples. In each MAD cohort, with the exception of the 1000 mg dose, study drug was administered once daily for ten consecutive days following an overnight fast at the same doses as in the SAD. The 1000 mg dose was administered for 8 days when, out of an abundance of caution, the dosing was interrupted due to a nonserious AE experienced by one subject. The event was later deemed to be unlikely related to study treatment by the investigator.

Relative Bioavailability Study An oral tablet formulation of icotrokinra was developed for use in Phase 2 clinical studies and a 200 mg tablet formulation was developed for use in ensuing Phase 3 clinical studies. The bioavailability study comparing the Phase 3 200 mg tablet formulation with the Phase 2 100 mg tablet formulation was conducted to bridge the two formulations. A single-dose, open-label, randomized, crossover study design was employed to evaluate icotrokinra bioavailability with the two formulations in healthy adult participants. A washout period of ≥ 7 days was included between treatment periods for each individual participant.

Participants

First-in-Human Study Healthy adult men and women of non-childbearing potential aged 18–65 years in good health (nonsmokers with no significant medical history or clinically significant laboratory abnormalities) and with a body mass index (BMI) of 18–32 kg/m^2 were eligible for inclusion. Key exclusion criteria were a history of clinically significant abnormalities or diseases; surgical resection of the stomach or small or large intestine; symptomatic infection; history of severe allergic or anaphylactic reactions; use of topical antibiotics; or a history of substance abuse.

Relative Bioavailability Study Healthy adult men or women (non-childbearing potential)

aged 18–60 years with a body weight ≥ 50 kg and BMI between 18 and 30 kg/m^2 deemed healthy on the basis of physical examination, medical history, and clinical laboratory tests were eligible for inclusion. A history of, or current, clinically significant medical illness excluded participation.

Pharmacokinetic Evaluation of Icotrokinra in Humans

First-in-Human Study PK parameters were assessed on Day 1 in SAD and Days 1 and 10 in the MAD study. Concentrations of icotrokinra in plasma from collected blood specimens were analyzed using a validated liquid chromatography with tandem mass spectrometry (LC–MS/MS) method. Following extraction from urine, feces, rectum, and sigmoid colon samples using standard procedures, icotrokinra concentrations were analyzed using a high-performance LC system coupled to an API4000 mass detector. PK analysis was done using Phoenix™ WinNonlin® (Certara LP) and were summarized using descriptive statistics. Icotrokinra plasma concentration–time data were graphically presented per treatment.

Icotrokinra dose proportionality was assessed using the power model with natural log-transformed PK parameter values and natural log-transformed dose (excluding the placebo group) using equation: ln (PK parameter) = $\beta_0 + \beta$ ln(dose) + ε. The power model was used to estimate the slope parameter (β) and the 90% confidence interval (CI) for the slope. Dose proportionality was concluded if the 90% CI of the slope estimate included the value of 1.

Relative Bioavailability Study The full PK profile of icotrokinra was determined over 48 h post-administration in each treatment period. Icotrokinra concentrations in plasma samples were determined using a validated LC–MS/MS method. PK analysis was done using Phoenix™ WinNonlin® (Certara LP) and were summarized using descriptive statistics.

In both the first-in-human (FIH) and relative bioavailability studies, safety was evaluated throughout each study via physical examination findings, vital signs, electrocardiograms, and clinical laboratory parameters and monitoring of AEs and serious AEs (SAEs).

Ethical Approval

Rat study protocols and procedures were conducted under the United Kingdom Home Office project license number PP9376768 that controls scientific procedures on animals in the United Kingdom under the Animals (Scientific Procedures) Act 1986. The regulations conform to the European Convention for the Protection of Vertebrate Animals Used for Experimental and Other Scientific Purposes (Strasbourg, Council of Europe) and achieve the standard of care required by the United States Department of Health and Human Services' Guide for the Care and Use of Laboratory Animals. Monkey study protocols and procedures were reviewed and approved by the Charles River (Nevada) Institutional Animal Care and Use Committee and were conducted in compliance with applicable sections of the Final Rules of the Animal Welfare Act regulations (Code of Federal Regulations, Title 9), the Public Health Service Policy on Humane Care and Use of Laboratory Animals from the Office of Laboratory Animal Welfare, the Guide for the Care and Use of Laboratory Animals from the National Research Council.

The FIH study protocol was reviewed and approved by Alfred Hospital Ethics Committee (Project 613/20 HREC/69080/Alfred-2020). The Human Research Ethics Committee (HREC) gave written approval for the Phase 1 FIH study in accordance with local regulations. The HREC was appropriately constituted and operated in accordance with the Notes for Guidance on Good Clinical Practice (GCP, CPMP/ICH/15/95), as adopted by the Australian Therapeutic Goods Administration (TGA, 2000) and the National Health and Medical Research Council (NHMRC) National Statement on Ethical Conduct in Human Research (2007, updated 2018). Each subject gave informed consent at the screening visit to participate in the study and publication. This study was conducted in accordance with the principles of the current

Declaration of Helsinki (Ethical Principles for Medical Research Involving Human Subjects), the NHMRC National Statement on Ethical Conduct in Human Research (2007, updated 2018), and Notes for Guidance on GCP (CPMP/ICH/135/95) established from the International Conference on Harmonization guidelines and adopted by the Australian TGA (2000). All study investigations were undertaken by scientifically and medically qualified persons.

The relative bioavailability study protocol was reviewed and approved by FAGG (federal agency for medicines and health products in Belgium; reference number R&D/1317536). The study was conducted in accordance with the ethical principles that have their origin in the Declaration of Helsinki and that are consistent with GCPs and applicable regulatory requirements. Informed consent was gained prior to the commencement of any study procedures.

RESULTS

In Vitro Characterization

Permeability Assessment in LLC-PK1 Cell Monolayers

Across the studied concentration range (1–300 µM), icotrokinra exhibited low permeability that was not saturable in polarized cell monolayer models expressing MDR1, the gene encoding human P-glycoprotein (P-gp), with apparent permeability coefficient $(P_{app})_{(A\text{-}B)}$ ranging from 0.90 to 1.96 nm/s and $P_{app\ (B\text{-}A)}$ from 0.61 to 1.98 nm/sec (Supplementary Table S1). Efflux ratios (ERs) were < 2 across the concentration range in the absence (0.7–1.2) or presence (1.1–1.3) of the P-gp inhibitor, valspodar, confirming no directional differences in permeability and no change in permeability with P-gp inhibition, indicating that icotrokinra is not a substrate of P-gp. Under the same incubation conditions, ERs of [^{14}C]-icotrokinra were also < 2 in mock-transfected cell monolayers.

Plasma Protein Binding and Blood Cell Partitioning

Icotrokinra showed low protein binding across species (Supplementary Table S2), with mean percent bound ranging between 43.7% and 56.0% in mouse, rat, and monkey plasma and 49.7–55.2% in human plasma. Protein binding was notably higher in rabbit plasma (mean bound compound 70.3–71.9%). No concentration-dependent differences in protein binding were observed across the tested concentrations (0.01–1 µM). Additionally, icotrokinra was found to be stable in plasma at 37°C for up to 16 h. Mean percent binding values ranged from 25.7% to 35.9% for 4% human albumin, 1.07% to 10.6% for 0.07% AAG, and 7.56% to 8.53% for 0.14% AAG, whereas in mixtures of 4% albumin with 0.07% or 0.14% AAG, percent binding ranged from 25.8% to 37.1% and 20.0% to 33.8%, respectively. Thus, icotrokinra appeared to be preferentially binding to human serum albumin as compared with AAG. Since plasma protein binding is low, no DDI related to plasma protein binding are expected.

Icotrokinra exhibited low blood partitioning and no preferential binding to RBCs, with mean observed $K_{WB/P}$ and $K_{RBC/P}$ values of < 1 in rat, dog, monkey, and human whole blood (Supplementary Table S3). Across icotrokinra concentrations of 2.5–250 ng/mL, mean $K_{WB/P}$ values ranged from 0.63 to 0.84 in rat, 0.61 to 0.84 in dog, 0.43 to 0.79 in monkey, and 0.49 to 0.61 in human whole blood after 2 h of incubation.

Metabolic Stability

Icotrokinra demonstrated in vitro stability in feces, GI mucosa, and hepatocytes across rat, monkey, and human species. At 50 µM, the mean half-life ($t_{1/2}$) values in fecal and GI mucosal matrices exceeded 24 h for all three species. After 24 h, the percentages of icotrokinra remaining in fecal homogenates relative to the initial concentrations were 81.3%, 75.2%, and 76.0% in rats, monkeys,

Table 1 Plasma pharmacokinetics of icotrokinra in rats and monkeys following intravenous or oral dosing

Dosing route	Animal	Dose, mg/kg	CL, mL/min/kg	V_{ss}, mL/kg	C_{max}, ng/mL	t_{max}, h	$AUC_{0-\infty}$, ng*h/mL	$t_{1/2}$, h	*F*, %
IV	Rat[a]	2	8.77 ± 0.387	459 ± 4.86	–	–	3,810 ± 166	0.762 ± 0.056	–
	Monkey[b,c]	1	1.44 ± 0.018	299 ± 30.4	–	–	12,000 ± 2930	3.47 ± 0.42	–
PO	Rat[a]	20	–	–	8.68 ± 3.10	2 (2, 2)[d]	44.2[e]	2.36[f]	0.12[e]
	Rat[a,g]	30	–	–	134	0.5	181	1.76	0.32
	Rat[a,g]	100	–	–	76.3	1	317	–[h]	0.17
	Rat[a,g]	300	–	–	134	1	1,120	–[h]	0.11
	Monkey[b]	2.5	–	–	11.0 ± 0.60	2 (1, 4)[d]	82.2 ± 25.2[e]	5.58 ± 3.86[e]	0.27[e]
	Monkey[b]	7.5	–	–	27.8 ± 5.86	1 (0.5, 1)[d]	226 ± 29.6[i]	6.41 ± 2.09[i]	0.25[i]
	Monkey[b]	22.5	–	–	84.3 ± 21.8	1.5 (1, 2)[d]	812 ± 302[i]	5.60 ± 2.02[i]	0.30[i]

Values are presented as mean ± standard deviation except as noted

$AUC_{0-\infty}$ area under the plasma concentration–time curve from time zero extrapolated to infinity, *CL* clearance, *C_{max}* maximum plasma concentration, *F* bioavailability, *h* hour, *IV* intravenous, *PK* pharmacokinetic, *PO* per os (oral gavage), *$t_{1/2}$* plasma elimination half-life, *t_{max}* time to reach maximum plasma concentration, *V_{ss}* volume of distribution at steady state

[a]Sprague Dawley rat ($N = 3$)

[b]Cynomolgus monkey ($N = 4$)

[c]$N = 3$: One animal showed an extravascular administration profile rather than a typical IV PK profile and thus was excluded from PK analysis

[d]Median (min, max)

[e]$N = 2$: Other animal(s) did not have sufficient data in elimination phase

[f]$N = 1$: Other animals did not have sufficient timepoints for $t_{1/2}$ estimation

[g]For rats dosed orally at 30, 100, and 300 mg/kg, sparse sampling was used, with 3 rats/timepoint, and composite profiles were used for PK parameter estimation

[h]Insufficient elimination phase to calculate $t_{1/2}$

[i]$N = 3$: One animal did not give sufficient data in elimination phase

and humans, respectively (Supplementary Figure S1a). The respective percentages remaining in GI tissues at 24 h ranged between 92.2% and 100% across species (Supplementary Figure S1b). Icotrokinra was also shown to be stable in SGF alone and solutions containing purified GI enzymes, including chymotrypsin, pancreatin, pepsin, and trypsin, with mean $t_{1/2}$ values exceeding 24 h and percentages of icotrokinra remaining after 24 h ranging between 84.4% and 100% across matrices (Supplementary Figure S1c). Icotrokinra turnover was low when incubated with hepatocytes, with mean $t_{1/2} > 371$ minutes (min) (> 6 h) and intrinsic clearance (CL_{int}) < 1.8 µL/min/10^6 cells. After 2 h of hepatocyte incubation, icotrokinra remained largely unchanged, with 95.7%, 92.8%, and 96.6% of the drug still present, in rat, monkey, and human hepatocytes, respectively, suggesting that it is not subject to significant hepatic metabolic clearance (Supplementary Figure S1d).

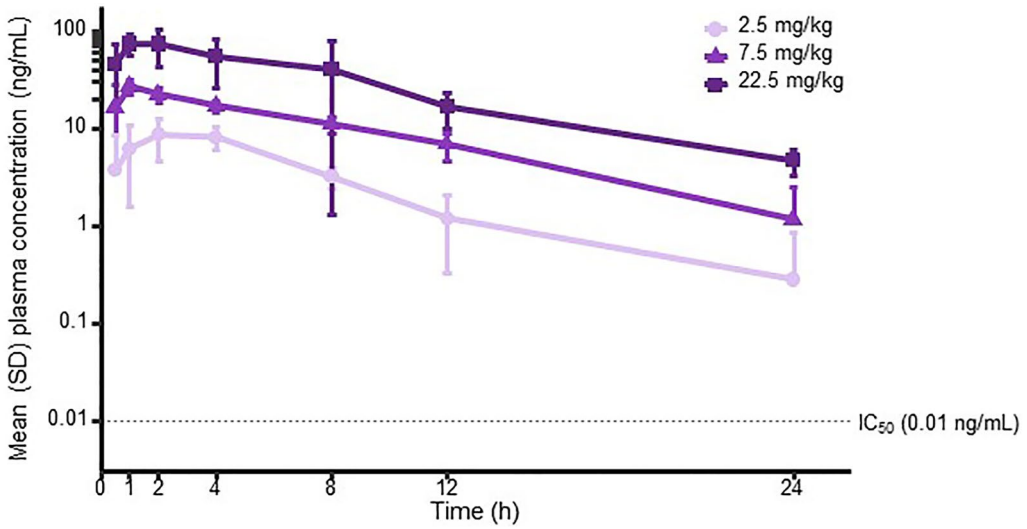

Fig. 2 Plasma concentrations of icotrokinra measured over 24 h in monkeys following a single oral administration. Dotted line represents the icotrokinra IC_{50} for IL-23-induced STAT3 phosphorylation in human PBMCs after 24 h [12]. SD values below 0 are not plotted. *h* hour, *IC_{50}* half-maximal inhibitory concentration, *IL* interleukin, *PBMC* peripheral blood mononuclear cell, *SD* standard deviation, *STAT3* signal transducer and activator of transcription 3

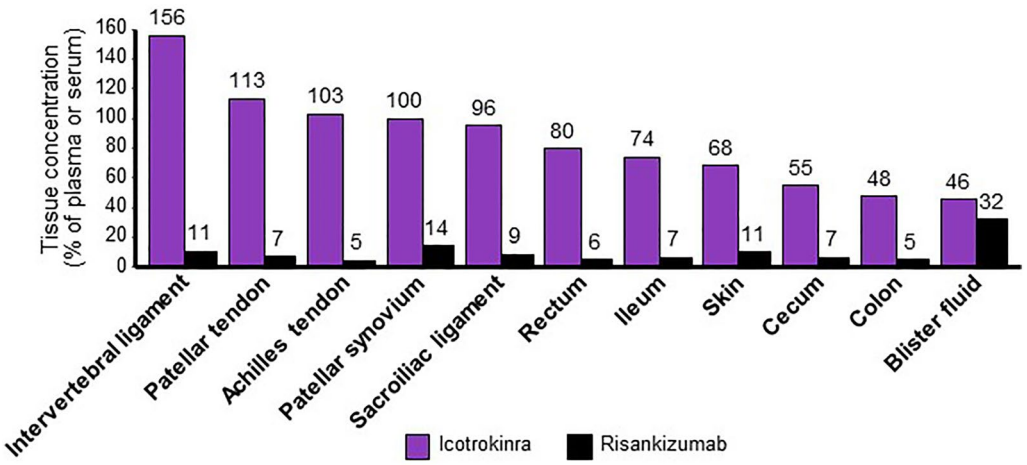

Fig. 3 Tissue distribution of icotrokinra (1 mL/kg intravenous) and risankizumab (2 mL/kg intravenous) in monkeys. Icotrokinra tissue concentration presented as tissue:plasma percentage. Risankizumab tissue concentration presented as tissue:serum percentage

Drug–Drug Interaction Studies

Icotrokinra was evaluated for its potential as a substrate and inhibitor of human transporters. Icotrokinra was not a substrate for P-gp, OATP1B1, OATP1B3, OAT1, OAT3, OCT2, MATE1, MATE2-K, and BCRP and did not inhibit P-gp, OAT1, OAT3, OCT2, MATE1, MATE2-K, BCRP, or BSEP activity (Supplementary Table S1; Supplementary Table S4;

Table 2 Mass balance of [^{14}C]-icotrokinra (300 mg/kg) and its main metabolites in rats (~ 400 µCi/kg) and monkeys (~ 100 µCi/kg) after oral administration

Analyte	Rat[a] (0–24 h), % of dose			Monkey[b] (0–96 h), % of dose		
	Feces	Urine	Total	Feces	Urine	Total
M5	–	–	–	0.89	–	0.89
M6	–	0.004	0.004	0.67	–	0.67
M7	–	0.028	0.028	–	0.06	0.06
M8	–	0.006	0.006	0.02	–	0.02
M9	–	0.034	0.034	–	0.02	0.02
M10	–	–	–	0.35	–	0.35
M11	–	–	–	–	0.02	0.02
M12	–	0.002	0.002	0.02	–	0.02
M13	–	–	–	0.02	–	0.02
M14	1.7	–	1.7	0.90	0.01	0.91
M16[c]	1.0	–	1.0	–	–	–
M25	–	0.010	0.010	–	–	–
M26	–	0.012	0.012	–	–	–
M27	–	0.003	0.003	–	–	–
UD	72.8	0.056	72.9	64.2	0.86	65.1
Sum	**75.5**	**0.155**	**75.7**	**67.1**	**0.97**	**68.1**

Values are presented as mean except as noted

h hour, *LC–MS/MS* liquid chromatography with tandem mass spectrometry, *M* metabolite, *UD* unchanged drug

[a]Sprague Dawley rat ($N = 2$)

[b]Cynomolgus monkey ($N = 2$)

[c]M16 estimated on the basis of LC–MS/MS data in rat

Supplementary Table S5; Supplementary Table S6). At the highest tested concentrations (measured concentrations of 24.7 µM for OATP1B1 and 24.2 µM for OATP1B3), 43.9% and 48.0% inhibition of OATP1B1 and OATP1B3 activity, respectively, were observed (Supplementary Table S4). No interaction with these transporters is anticipated at clinically relevant concentrations (the maximum plasma concentration [C_{max}] for a 200 mg dose is approximately 0.002 µM), suggesting icotrokinra would not influence the PK of drugs that are substrates of these transporters.

Icotrokinra (up to 100 µM) did not exhibit concentration-dependent inhibition of major human CYP enzymes. The half-maximal inhibitory concentration (IC_{50}) for all CYP isoforms was ≥ 100 µM, indicating minimal potential for CYP-mediated DDIs. At the highest concentration tested (100 µM), maximum inhibition was < 10% for most CYP isoforms, with only CYP1A2 (19%) and CYP2E1 (30%)

showing weak inhibition. These findings suggest icotrokinra is not a significant inhibitor of the selected CYP enzymes under the conditions tested.

The potential for icotrokinra to induce CYP1A2, CYP2B6, and CYP3A4 mRNA expression was evaluated in cultured human hepatocytes at concentrations of up to 90 µM. Icotrokinra caused no induction (< 2-fold change in mRNA expression) and minimal response relative to the positive control (< 5% at 90 µM; Supplementary Table S7), indicating no significant induction of the selected CYP enzymes under the conditions tested. Together with the hepatocyte stability and CYP inhibition results, these findings indicate icotrokinra has a low potential for enzyme-mediated DDIs.

In Vivo Pharmacokinetic Studies of Icotrokinra

Pharmacokinetic Profile in Rats and Monkeys

Following a single IV dose (2 mg/kg in rats, 1 mg/kg in monkeys), icotrokinra exhibited moderate distribution, with estimated volumes of distribution at steady state (V_{ss}) of 459 mL/kg in rats and 299 mL/kg in monkeys. The area under the plasma concentration–time curve from time 0 extrapolated to infinity ($AUC_{0-\infty}$) was 3810 ng*h/mL in rats and 12,000 ng h/mL in monkeys (Table 1). Plasma elimination $t_{½}$ was 0.762 h and 3.47 h in rats and monkeys, respectively, and mean clearance was 8.77 mL/min/kg and 1.44 mL/min/kg, respectively.

Oral administration of icotrokinra at 20, 30, 100, and 300 mg/kg in rats yielded a mean C_{max} of 8.68, 134, 76.3, and 134 ng/mL; oral bioavailability (F) of 0.12%, 0.32%, 0.17%, and 0.11%; and an $AUC_{0-\infty}$ of 44.2, 181, 317, and 1,120 ng*h/mL (Table 1). Terminal half-life was approximately 2 h where estimatable. Similar results were observed in monkeys following single oral doses of 2.5, 7.5, or 22.5 mg/kg, with plasma concentrations peaking 1–2 h post-dose (Table 1, Fig. 2); respective mean C_{max} values were 11.0, 27.8, and 84.3 ng/mL, demonstrating an approximately dose-proportional increase. Systemic exposure ($AUC_{0-\infty}$) increased dose-proportionally by 2.75-fold (7.5 versus 2.5 mg/kg) and 9.88-fold (22.5 versus 2.5 mg/kg) across tested dose levels. Oral bioavailability of icotrokinra in monkeys was low, with values of 0.27%, 0.25%, and 0.30% at doses of 2.5, 7.5, and 22.5 mg/kg, respectively. However, even at the lowest dose of 2.5 mg/kg, icotrokinra plasma concentrations exceeded its IC_{50} for inhibition of IL-23-induced signal transducer and activator of transcription 3 (STAT3) phosphorylation in human peripheral blood mononuclear cells (PBMCs; Fig. 2) [12]. Elimination $t_{½}$ was consistent across the oral dose groups, ranging from 5.6 h to 6.4 h (Table 1).

Tissue Distribution in Monkeys

In monkeys, IV-administered icotrokinra (1 mg/kg) was found to be well distributed to tissues relevant to psoriasis, psoriatic arthritis, and IBD, including skin, joints, and GI tissues (Fig. 3). Skin, blister fluid, ileum, cecum, colon, rectum, patellar synovium, patellar tendon, intervertebral ligament, Achilles tendon, and sacroiliac ligament had estimated tissue concentrations relative to plasma (tissue:plasma) between 45.8% and 156%. Risankizumab, a monoclonal antibody that inhibits the IL-23 cytokine, showed tissue concentrations relative to serum (tissue:serum) ranging from 4.07% to 32.1% after a 1 mg/kg IV dose in monkeys, using the same testing site and collection procedures, with timepoints adjusted accordingly for the peptide and antibody (Fig. 3).

Metabolic Profiling in Rats and Monkeys

Following oral administration of [^{14}C]-icotrokinra at 300 mg/kg in rats, unchanged icotrokinra was the predominant species (> 95%) in all plasma samples. Eight metabolites (M6, M7, M8, M9, M12, M25, M26, and M27), along with unchanged icotrokinra, were identified in urine at comparable levels (Table 2). In feces, unchanged icotrokinra was the dominant species (96.3%), with minor contributions from metabolites M14 (2.2%) and M16 (1.5%). The recovery of unchanged drug from feces (0–24 h) was on average 72.8% of the total dose (Table 2). M27 and M16 were

Table 3 Baseline characteristics in Phase 1 healthy volunteers

Characteristic									
First-in-human study									
SAD									
	10 mg (*N* = 6)	**25 mg (*N* = 6)**	**100 mg (*N* = 5)**	**300 mg (*N* = 6)**	**1000 mg (*N* = 6)**	**Overall (*N* = 29)**	**Placebo (*N* = 10)**	**Total (*N* = 39)**	
Age, years	21.5 (18, 23)	24.0 (19, 52)	31.0 (23, 52)	28.0 (20, 34)	21.5 (20, 42)	23.0 (18, 52)	23.0 (19, 41)	23.0 (18, 52)	
Sex, *n* (%)									
Male	6 (100)	6 (100)	5 (100)	6 (100)	6 (100)	29 (100)	10 (100)	39 (100)	
Female	0	0	0	0	0	0	0	0	
Race, *n* (%)									
Asian	1 (16.7)	4 (66.7)	2 (40.0)	1 (16.7)	4 (66.7)	12 (41.4)	5 (50.0)	17 (43.6)	
Black or African American	0	0	0	2 (33.3)	0	2 (6.9)	0	2 (5.1)	
White	5 (83.3)	2 (33.3)	3 (60.0)	3 (50.0)	2 (33.3)	15 (51.7)	5 (50.0)	20 (51.3)	
Weight, kg	76.2 (69, 112)	69.0 (56, 74)	78.6 (62, 94)	76.5 (62, 79)	73.2 (70, 108)	73.9 (56, 112)	71.7 (62, 85)	73.5 (56, 112)	
Height, cm	182 (172, 190)	172 (167, 181)	177 (169, 182)	176 (174, 185)	178 (171, 189)	177.0 (167, 190)	178 (172, 185)	177 (167, 190)	
BMI, kg/m^2	22.6 (22, 32)	23.3 (19, 26)	25.1 (22, 29)	24.1 (20, 26)	24.6 (23, 31)	24.0 (19, 32)	22.4 (20, 28)	23.7 (19, 32)	
MAD									
	10 mg (*N* = 8)	**25 mg (*N* = 4)**	**100 mg (*N* = 8)**	**300 mg (*N* = 8)**	**1000 mg (*N* = 8)**	**100 mg (*N* = 8)[a]**	**Overall (*N* = 44)**	**Placebo (*N* = 12)**	**Total (*N* = 56)**
Age, years	26.5 (22, 52)	25.5 (25, 47)	27.0 (20, 49)	28.0 (19, 35)	29.5 (23, 56)	32.5 (19, 53)	28.0 (19, 56)	27.5 (24, 40)	28.0 (19, 56)
Sex, *n* (%)									
Male	8 (100.0)	4 (100.0)	8 (100.0)	8 (100.0)	8 (100.0)	8 (100.0)	44 (100.0)	12 (100.0)	56 (100)
Female	0	0	0	0	0	0	0	0	0
Race, *n* (%)									
Asian	1 (12.5)	2 (50.0)	1 (12.5)	4 (50.0)	1 (12.5)	1 (12.5)	10 (22.7)	6 (50.0)	16 (28.6)

Table 3 continued

MAD									
	10 mg (*N* = 8)	**25 mg (*N* = 4)**	**100 mg (*N* = 8)**	**300 mg (*N* = 8)**	**1000 mg (*N* = 8)**	**100 mg (*N* = 8)[a]**	**Overall (*N* = 44)**	**Placebo (*N* = 12)**	**Total (*N* = 56)**
White	7 (87.5)	2 (50.0)	5 (62.5)	4 (50.0)	7 (87.5)	6 (75.0)	31 (70.5)	6 (50.0)	37 (66.1)
Other	0	0	2 (25.0)	0	0	1 (12.5)	3 (6.8)	0	3 (5.4)
Weight, kg	76.5 (61, 84)	75.0 (53, 96)	91.7 (75, 99)	81.7 (65, 99)	80.9 (60, 104)	79.5 (61, 92)	80.8 (53, 104)	73.9 (58, 98)	79.5 (53, 104)
Height, cm	175 (169, 189)	176 (168, 185)	180 (174, 188)	174 (171, 180)	180 (163, 186)	177 (166, 192)	177 (163, 192)	168 (163, 188)	177 (163, 192)
BMI, kg/m^2	23.1 (20, 30)	23.7 (18, 29)	26.6 (24, 32)	27.3 (21, 32)	25.4 (20, 30)	25.4 (19, 31)	25.4 (18, 32)	24.1 (20, 29)	25.2 (18, 32)

Relative bioavailability	
	***N* = 24**
Age years	55.0 (23.0, 60.0)
Sex, *n* (%)	
Male	19 (79.2)
Female	5 (20.8)
Race, *n* (%)	
Asian	1 (4.20)
White	23 (95.8)
Weight, kg	79.7 (60, 91)
Height, cm	174 (152, 193)
BMI, kg/m^2	26.0 (22, 30)

Values are presented as median (minimum, maximum) except as noted

BMI body mass index, *MAD* multiple ascending dose, *SAD* single ascending dose

[a]Cohort was added for sigmoidoscopy assessments

detected in the spiked blank plasma, feces, and urine samples, indicating that the presence of these metabolites could be partially attributed to sample processing.

Following a single oral dose of [^{14}C]-icotrokinra at 300 mg/kg in monkeys, unchanged drug was the predominant species in plasma, and the main species recovered in the excreta, corresponding to 64.2% of dose recovery. In feces, metabolites (M5, M6, M8, M10, M12, M13, and M14) accounted for very low amounts of the oral dose (Table 2). Four metabolites (M7, M9, M11, and M14) and unchanged icotrokinra were detected in urine at similarly low levels (Table 2).

Table 4 Summary of icotrokinra PK parameters in Phase 1 healthy volunteers

PK parameter												
SAD												
	10 mg (*N* = 6)		**25 mg (*N* = 6)**		**100 mg (*N* = 5)**		**300 mg (*N* = 6)**		**1000 mg (*N* = 6)**			
C_{max}, ng/mL	0.17 ± 0.09		0.79 ± 0.55		1.48 ± 0.41		3.97 ± 1.87		12.23 ± 5.66			
$t_{max,}$ h, median (min, max)	2.50 (1.0, 5.0)		1.50 (0.5, 5.0)		3.00 (2.0, 6.0)		4.00 (3.0, 8.0)		3.50 (1.0, 6.0)			
$AUC_{0\text{-last}}$, ng*h/mL	1.30 ± 0.74		6.10 ± 2.88		19.3 ± 5.17		49.5 ± 20.1		152 ± 24.0			
$AUC_{0-\infty}$, ng*h/mL	1.56 ± 0.73		6.47 ± 2.78		20.7 ± 6.50		51.0 ± 20.6		156 ± 23.5			
$t_{½}$, h	4.95 ± 0.54		8.54 ± 2.36		11.7 ± 5.43		9.64 ± 1.34		8.73 ± 1.26			
CL/F, L/h	7430 ± 2630		4530 ± 1950		5230 ± 1690		7070 ± 3690		6530 ± 1050			
V_z/F, L	52,500 ± 18,900		59,900 ± 43,600		84,300 ± 30,800		95,600 ± 43,400		83,400 ± 23,500			
MAD												
	10 mg (*N* = 8)		**25 mg (*N* = 4)**		**100 mg (*N* = 8)**		**300 mg (*N* = 8)**		**1000 mg (*N* = 8)**		**100 mg (*N* = 8)[b]**	
	Day 1	**Day 10**	**Day 1**	**Day 10**	**Day 1**	**Day 10**	**Day 1**	**Day 10**	**Day 1**	**Day 10[a]**	**Day 1**	**Day 10**
C_{max}, ng/mL	0.14 ± 0.06	0.19 ± 0.06[c]	0.57 ± 0.28	0.55 ± 0.23	3.34 ± 3.78	1.62 ± 0.77[c]	5.81 ± 5.61	5.28 ± 2.07	16.6 ± 26.3	–	1.11 ± 0.40	1.23 ± 0.69
t_{max}, h, median (min, max)	4.0 (1.0, 8.0)	4.0 (0.5, 5.0) [c]	1.5 (0.5, 5.0)	1.0 (0.5, 1.0)	1.5 (0.25, 8.0)	6.0 (2.0, 8.0)[c]	3.5 (1.0, 8.0)	1.0 (0.5, 6.0)	5.0 (0.5, 6.0)	–	4.5 (1.0, 6.0)	2.0 (0.5, 12.0)
AUC_{0-24h}, ng*h/mL	1.42 ± 0.41[c]	1.96 ± 0.45[c]	4.74 ± 0.90	5.19 ± 1.50	21.8 ± 13.9	17.7 ± 5.76[c]	52.1 ± 33.7	53.4 ± 14.6	145 ± 162	–	11.1 ± 3.53	12.7 ± 5.56
AI AUC	–	1.49 ± 0.29[d]	–	1.13 ± 0.42	–	0.91 ± 0.33[c]	–	1.18 ± 0.41	–	–	–	1.16 ± 0.43
AI C_{max}	–	1.65 ± 0.99[c]	–	1.17 ± 0.78	–	0.70 ± 0.36[c]	–	1.20 ± 0.52	–	–	–	1.12 ± 0.47
$t_{½}$, h	–	10.6 ± 5.01[c]	–	15.7 ± 7.66	–	9.95 ± 2.05[c]	–	8.86 ± 1.68	–	–	–	10.1 ± 4.07
CL/F, L/h	–	5380 ± 1450[c]	–	5210 ± 1830	–	6320 ± 2500[c]	–	6100 ± 2100	–	–	–	9740 ± 5000
V_z/F, L	–	83,900 ± 59,400[c]	–	132,000 ± 116,000	–	88,900 ± 32,300[c]	–	76,300 ± 24,500	–	–	–	160,000 ± 143,000
Relative bioavailability												
					1 × 200 mg tablet (*N* = 24)							**2 × 100 mg tablets (*N* = 23)**
C_{max}, ng/mL					3.62 ± 1.48							4.56 ± 3.05

Table 4 continued

Relative bioavailability		
	1 × 200 mg tablet (*N* = 24)	**2 × 100 mg tablets (*N* = 23)**
t_{max}, h, median (min, max)	2.00 (0.25, 8.00)	2.00 (0.25, 5.00)
$AUC_{0-24\,h}$, ng*h/mL	34.6 ± 9.09	37.9 ± 12.9
AUC_{0-last}, ng*h/mL	42.0 ± 10.7[e]	45.3 ± 15.5
$AUC_{0-\infty}$, ng*h/mL	44.8 ± 11.4[e]	47.9 ± 16.0
$t_{1/2}$, h	13.0 ± 4.1	12.4 ± 3.5

Values are presented as mean ± standard deviation except as noted

AI AUC accumulation index for area under the curve estimated as the ratio of $AUC_{0-24\,h}$ on Day 10 to AUC_{0-24h} on Day 1, *AI* C_{max} accumulation index for C_{max} estimated as the ratio of C_{max} on Day 10 to C_{max} on Day 1, *AUC* area under the plasma concentration–time curve, $AUC_{0\text{-}24h}$ AUC from time zero to 24 h, $AUC_{0-\infty}$ AUC from time zero extrapolated to infinity, AUC_{0-last} AUC from time zero to the time of the last measurable concentration, *CL/F* apparent total body clearance, C_{max} maximum plasma concentration, *h* hour, *MAD* multiple ascending dose, *PK* pharmacokinetic, *SAD* single ascending dose, t_{lag} time of the first measurable concentration, t_{max} time to reach maximum plasma concentration, $t_{½}$ plasma elimination half-life, *Vz/F* apparent volume of distribution

[a]Dosing was stopped on Day 8

[b]Cohort with sigmoidoscopy assessments

[c]$N = 7$

[d]$N = 6$

[e]$N = 23$

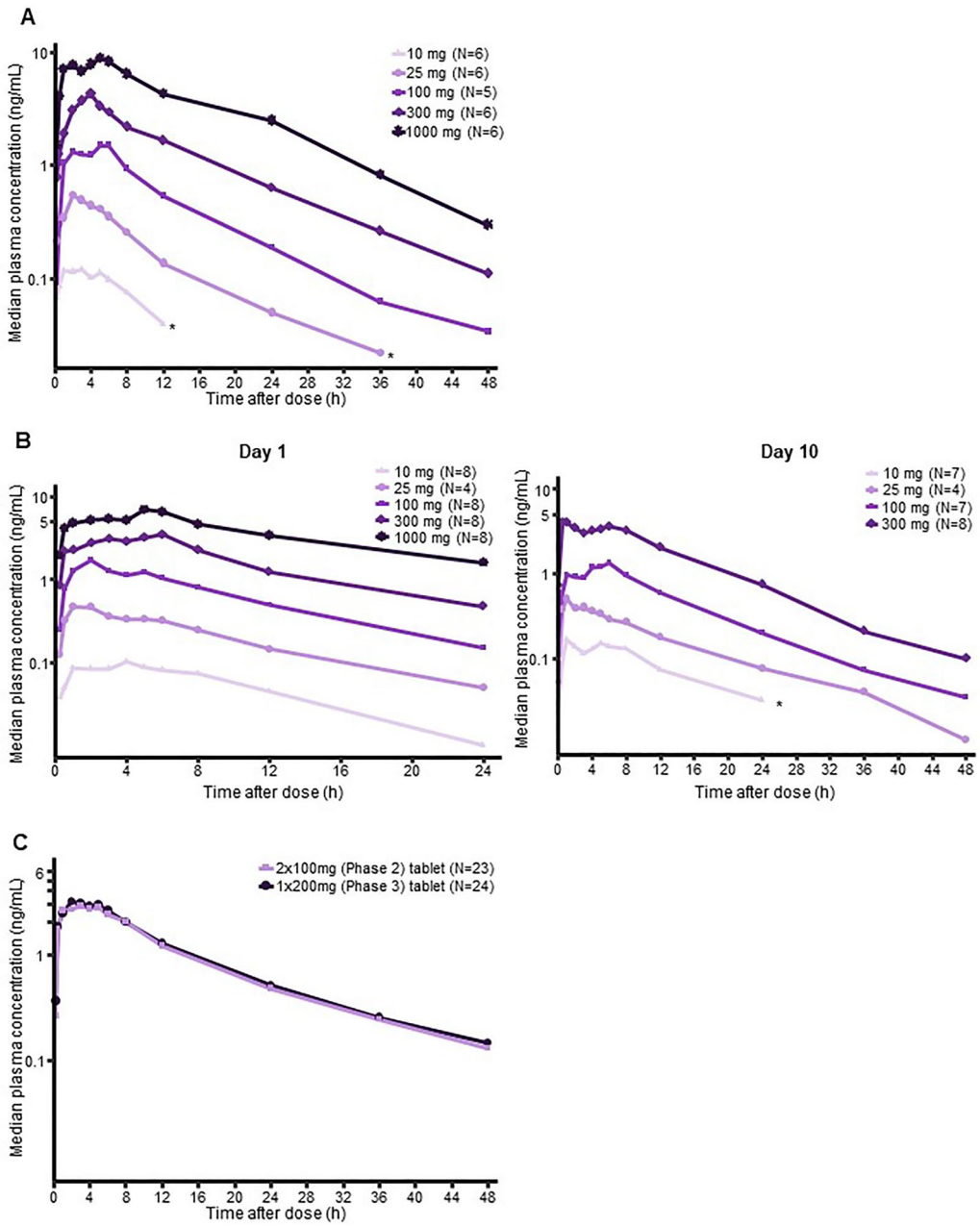

Fig. 4 Plasma concentrations of icotrokinra in healthy participants following a single dose (**A**) or multiple doses at Days 1 and 10 (**B**) of the solution formulation, and comparing 1 × 200 mg (Phase 3) tablet with 2 × 100 mg (Phase 2) tablets (**C**). *Data below the level of quantification are not plotted. The 1000 mg dose was administered for 8 days only. *h* hour

Excretion in Rats and Monkeys

Following an oral dose of 300 mg/kg [^{14}C]-icotrokinra, fecal excretion was the primary route of elimination in both rats (96.8% recovered) and monkeys (67.0% recovered) within 96 h, with the majority eliminated in the first 24 h (Supplementary Table S8). Total recovery of the dose over 96 h, including from urine, feces, and cage washing, was 97.3% in

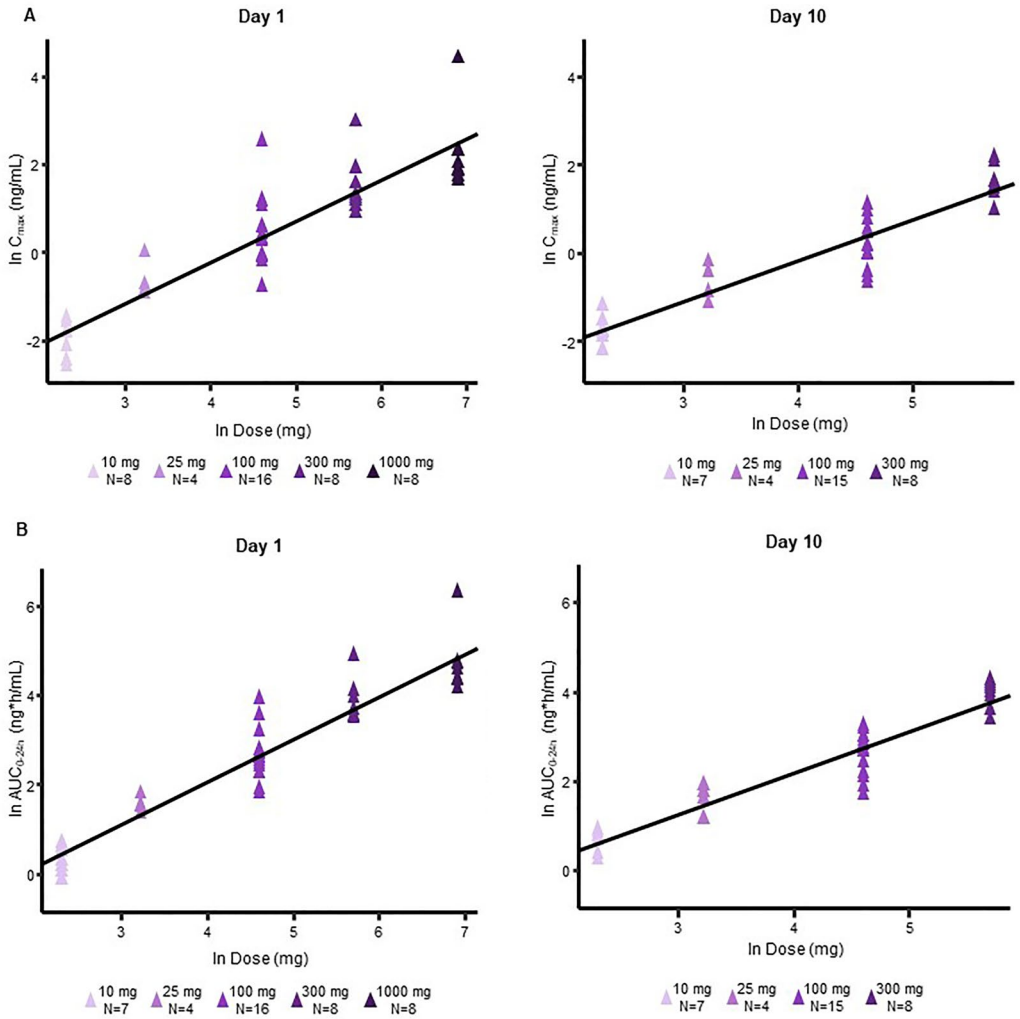

Fig. 5 Maximum plasma concentration (**A**) and area under the plasma concentration–time curve at 24 h (**B**) following multiple doses of icotrokinra in healthy participants. Dose proportionality was assessed using the power model with natural log-transformed PK parameter values and natural log-transformed dose (excluding the placebo group). Line represents best fit on the basis of linear regression analysis. AUC_{024h} area under the curve at 24 h, C_{max} maximum plasma concentration, *ln* natural log, *PK* pharmacokinetic

rats and 73.1% in monkeys. In both rats and monkeys, < 1% of icotrokinra was recovered from urine within 96 h; however, this likely represents a major clearance pathway for systemically absorbed drug since the oral bioavailability is similarly low. Quantitative whole-body autoradiography of a single monkey carcass revealed that icotrokinra levels were below the lower limit of quantification (LLOQ) in all tissues at 96 h post-dose, indicating negligible retention.

Icotrokinra Phase 1 Clinical Studies in Healthy Volunteers

Participant Disposition and Demographics

Baseline characteristics of healthy adults enrolled in the FIH study are presented in Table 3. All participants were men. In the SAD population, the median participant age was 23.0 years; 51.3% were white; and median

Table 5 Comparison of icotrokinra PK parameters following single administration of 200 mg icotrokinra in Phase 1 healthy volunteers in the relative bioavailability study

	Formulation	*N*	Geometric mean	Comparison	GMR, %	90% CI	Inter-participant CV, %	Intra-participant CV, %
C_{max}, ng/mL	1 × 200 mg tablet	24	3.40	1 × 200 mg tablet versus 2 × 100 mg tablet	88.1	74.3–104.4	26.7	35.6
	2 × 100 mg tablet	23	3.86					
AUC_{0-last}, ng*h/mL	1 × 200 mg tablet	23	41.1	1 × 200 mg tablet versus 2 × 100 mg tablet	94.2	85.1–104.3	21.0	20.5
	2 × 100 mg tablet	23	43.7					
$AUC_{0-\infty}$, ng*h/mL	1 × 200 mg tablet	23	43.8	1 × 200 mg tablet versus 2 × 100 mg tablet	94.9	85.6–105.2	19.6	20.7
	2 × 100 mg tablet	23	46.2					

PK parameters were log transformed and submitted to a linear mixed effects model controlling for intervention, sequence, and period as fixed effects, and participant within sequence as a random effect. Results are presented on original scale after antilogarithm transformation

AUC area under the plasma concentration–time curve, $AUC_{0-\infty}$ AUC from time zero extrapolated to infinity, AUC_{0-last} AUC from time zero to the time of the last measurable concentration, CI confidence interval, *CV* coefficient of variation, C_{max} maximum plasma concentration, *GMR* geometric mean ratio, *N* number of data included in the model, *PK* pharmacokinetic

weight and BMI were 73.5 kg and 23.7 kg/m^2, respectively. The median participant age in the MAD population was 28.0 years; 66.1% were white; and the median weight and BMI were 79.5 kg and 25.2 kg/m^2, respectively. In the MAD population, two participants withdrew consent for reasons unrelated to safety findings: one participant withdrew consent for participation and the other discontinued due to noncompliance.

Among the 24 healthy participants enrolled in the relative bioavailability study, 23 completed the study as planned; 1 participant discontinued the study due to a treatment-emergent AE (otitis media). The median age was 55.0 years, 79.2% were men, 20.8% women, and 95.8% were white (Table 3). The median weight and BMI were 79.7 kg and 26.0 kg/m^2, respectively.

Pharmacokinetic Profile in Humans

Limited PK of icotrokinra in humans has been previously reported for the SAD and MAD populations [12]. In the SAD population, following single oral dose administration of icotrokinra formulated as a solution, rapid absorption was observed, with a median time to reach maximum plasma concentration (t_{max}) ranging from 1.5 h to 4.0 h post-dose (Table 4). The mean $t_{1/2}$ ranged from approximately 9–12 h across dose cohorts (25–1000 mg). The median plasma concentrations of icotrokinra increased with increasing doses up to 1000 mg (Fig. 4A). In the MAD cohort, following multiple doses of icotrokinra formulated as a solution, the median t_{max} ranged from 1.5 h to 5.0 h on Day 1 and from 1.0 h to 6.0 h on Day 10 (Table 4). The mean $t_{1/2}$ was

approximately 9–16 h. Consistent with the half-life, a comparison of C_{max} and AUC from time 0 to the time of the last measurable concentration ($AUC_{0–last}$) values on Days 1 and 10 indicated an accumulation ratio of 0.70–1.65-fold for C_{max} and 0.9–1.49-fold for AUC with once-daily multiple dosing. Also following multiple doses, the median plasma concentrations on Days 1 and 10 exhibited a dose-dependent increase (Fig. 4B). A dose-proportional increase was also seen for both mean C_{max} (Fig. 5A) and AUC from time 0 h to 24 h ($AUC_{0–24\ h}$; Fig. 5B). The slopes (linear coefficients) for C_{max} and $AUC_{0–24\ h}$ on Day 1 and Day 10 were close to unity, and the 90% CIs included unity.

In the relative bioavailability study, a median t_{max} of 2 h was observed following a single oral dose of 200 mg icotrokinra, formulated as 1 × 200 mg (Phase 3) or 2 × 100 mg (Phase 2) tablets, under fasted conditions (Table 4). The mean $t_{1/2}$ was also consistent across formulations, with values ranging from 12.4 h to 13.0 h. After reaching a maximum, plasma concentrations of icotrokinra exhibited a biphasic decline with both the 1 × 200 mg (Phase 3) and 2 × 100 mg (Phase 2) tablets (Fig. 4C). Point estimates of the geometric mean ratios (GMRs) indicated that the relative bioavailability of icotrokinra for the 1 × 200 mg (Phase 3) tablet compared with the 2 × 100 mg (Phase 2) tablets was 88.1% for C_{max}, 94.2% for $AUC_{0–last}$, and 94.9% for $AUC_{0–\infty}$ (Table 5).

Metabolic Profiling and Excretion in Humans

Unchanged icotrokinra was the only drug-related material detected in plasma across both the SAD and MAD populations. Urinary excretion of unchanged icotrokinra was negligible (< 0.001%), while fecal excretion of unchanged icotrokinra increased with dose, ranging from 37.2% at 10 mg to 80.7% at 1000 mg. No metabolites were detected in plasma or urine. Detectable concentrations of icotrokinra were noted in sigmoid colon and rectal biopsy samples collected from participants following 25 mg and 100 mg icotrokinra doses.

Overall, no SAEs were reported and findings from safety assessments in the FIH were as those reported previously [12].

DISCUSSION

This report describes, for the first time, the ADME of icotrokinra, a first-in-class targeted oral peptide that selectively blocks IL-23R signaling. Historically, most peptide therapeutics have been administered via parenteral routes. Orally administered peptides face several barriers to absorption in the GI tract. First, the highly acidic pH of the stomach (< 2) [15] can result in hydrolysis or destabilization of the three-dimensional peptide structure [16]. In the intestine, peptides can be degraded by high levels of proteolytic enzymes, as well as enzymes from intestinal flora, which efficiently break peptide bonds. Additionally, peptides generally do not adhere to Lipinski's "rule of five" parameters, which define the optimal chemical space for oral absorption [17]. Factors such as high molecular weight and low lipophilicity result in very low intestinal permeability for most peptides.

More recently, several strategies have been implemented to improve oral bioavailability of peptides by increasing their proteolytic stability and permeability. To support the discovery of such compounds, new screening strategies, such as those described in this publication, have been employed. These include stability assays that use proteolytic enzymes, mucosal homogenates, and other GI matrices rather than the typical liver-derived systems that are standard for optimizing the stability of small molecule therapeutics. Furthermore, due to a lack of clearly defined regulatory guidelines for assessing DDI of peptides, small-molecule regulatory guidance is often followed [18]. Herein, the strategies described above were used to assess the stability of icotrokinra and characterize its ADME and DDI properties.

The results of ADME profiling demonstrated that icotrokinra has high metabolic stability, low risk for transporter- and enzyme-mediated DDIs, and distributes widely in tissues. In vitro

absorption assays found icotrokinra is not a substrate or inhibitor of P-gp or other drug transporters, indicating it should not interfere with the transport of substrate drugs across membranes. Additionally, icotrokinra is not cleared hepatically and does not inhibit or induce CYP enzymes, suggesting it should not interfere with metabolism or clearance of other drugs. Oral bioavailability was relatively low, which is typical of peptides [19]; however, drug levels detected in plasma were substantial, without the use of absorption enhancers, and previous studies have demonstrated the ability of these concentrations to significantly reduce IL-23-stimulated IFNγ production in human blood [12]. Icotrokinra distributes well to tissues implicated in psoriasis, psoriatic arthritis, and IBD. In monkeys, the estimated tissue concentrations of icotrokinra ranged between 46% and 156% of plasma concentrations following a single IV dose, compared with 4–27% of serum concentrations for the anti-IL-23 antibody risankizumab. The observed risankizumab tissue distribution profile is also consistent with typical antibody biodistribution coefficients reported in the literature, ranging from 5% for intestine to 16% for skin [20, 21]. Icotrokinra is not subject to significant hepatic metabolic clearance, as demonstrated by in vitro experiments in rat, monkey, and human hepatocytes, which revealed low drug turnover, with drug remaining largely unchanged after 2 h. Additionally, minimal metabolism of icotrokinra was noted in vivo in rats and monkeys, with the majority of icotrokinra being excreted in feces as unchanged drug. The main route of excretion for unabsorbed icotrokinra is through fecal elimination, while absorbed drug is likely cleared by the kidneys [16]. Together, these results represent a typical ADME profile for a peptide [22], with the exception that icotrokinra, due to its structural design, exhibited higher stability than generally observed for peptides administered orally [23]. The high stability and potency of icotrokinra, lack of interaction with transporters, and broad tissue distribution relative to monoclonal antibodies allows the drug to be sufficiently bioavailable and to produce systemic effects.

The nonclinical PK profile of icotrokinra translated well to its human PK. In the Phase 1 FIH study, an approximately dose-proportional increase in the plasma concentrations with increasing icotrokinra dose was observed. Minimal drug accumulation following once daily multiple dosing was noted, consistent with the half-life of icotrokinra. Intact icotrokinra was primarily excreted in the feces with low amounts of unchanged drug found in urine. The bioavailability of the 200 mg (Phase 3) tablet was comparable to that of the 100 mg (Phase 2) tablet.

Monoclonal antibodies targeting IL-23 have exhibited favorable safety profiles in long-term clinical and real-world studies [24–27], underscoring the feasibility of modulating the IL-23 signaling pathway for the treatment of chronic inflammatory diseases. No safety signals were identified following single- and multiple-dose administrations of icotrokinra as a solution formulation (10–1000 mg) and as an oral tablet (100–200 mg) [13, 14].

The present study data have some limitations. Due mainly to ethical issues, the sample size and number of timepoints analyzed for the monkey tissue distribution and comparison with risankizumab were limited. The animal tissue PK data have not been directly tied to PK and efficacy readouts in humans. Considering that peptides are cleared by proteolytic enzymes throughout the body, rather than strictly via cytochrome P450 enzymes in the liver, available in vitro assays for this modality are not as standardized as the assays used for small molecules. For example, the specific enzymes that degrade icotrokinra to metabolites could not be fully characterized, as they typically would be for a small molecule. Due to the high capacity of proteolytic enzymes, DDI involving these pathways are unlikely to occur.

CONCLUSIONS

Overall, these findings indicate that icotrokinra is a stable and bioavailable first-in-class targeted oral peptide that potently and selectively blocks IL-23R signaling, thus supporting its further assessment in clinical settings. No DDI risk has been identified on the basis of in vitro data and the peptide modality. The Phase 3

ICONIC development program has been initiated to evaluate the safety and efficacy of icotrokinra in broad populations of adults with moderate-to-severe plaque psoriasis with the ICONIC-LEAD (NCT06095115), ICONIC-TOTAL (NCT06095102), ICONIC-ADVANCE 1 (NCT06143878), and ICONIC-ADVANCE 2 (NCT06220604) studies currently ongoing.

ACKNOWLEDGEMENTS

The authors would like to thank Teddy Kosoglou (former Johnson & Johnson employee) for his contribution to this project and would also like to thank the participants of the study.

Medical Writing, Editorial and Other Assistance. Medical writing support was provided by JSS Medical Research, Inc, under the direction of the authors in accordance with Good Publication Practice guidelines (Ann Intern Med. 2022;175:1298–1304), and funded by Johnson & Johnson.

Author Contribution. All authors meet the International Committee of Medical Journal Editors criteria for authorship of this article, were involved in drafting the article or revising it critically for important intellectual content and approved the final version to be published. Beverly Knight, Brinda Tammara, Nishit B Modi, Shannon Dallas, Saro Mardirosian, Jianyao Wang, Aline Laenen, Laurent Leclercq, Karen DiLoreto, Lieve Adriaenssen, Darren Moss, David Polidori, Siladitya Ray Chaudhuri, Seonghee Park, Carlo Sensenhauser, Anthony Ndifor, Siddharth Sukumaran, Tristan Baguet, Yifan Shi, Shefali Patel, Brian Geist, Mario Monshouwer had full access to all the data in the study and take responsibility for the integrity of the data and the accuracy of the data analysis. Study conception and design: Beverly Knight, Brinda Tammara, Nishit B Modi, Shannon Dallas, Saro Mardirosian, Jianyao Wang, Aline Laenen, Laurent Leclercq, Karen DiLoreto, Lieve Adriaenssen, Darren Moss, David Polidori, Siladitya Ray Chaudhuri, Seonghee Park, Carlo Sensenhauser, Siddharth Sukumaran, Tristan Baguet, Yifan Shi, Shefali Patel, Brian Geist, Anne Fourie, Raymond Patch, Chengzao Sun, Stephanie A Barros, Sandeep Somani, Mario Monshouwer. Acquisition of data: Beverly Knight, Brinda Tammara, Nishit B Modi, Shannon Dallas, Saro Mardirosian, Jianyao Wang, Aline Laenen, Laurent Leclercq, Karen DiLoreto, Lieve Adriaenssen, Darren Moss, David Polidori, Siladitya Ray Chaudhuri, Seonghee Park, Carlo Sensenhauser, Siddharth Sukumaran, Tristan Baguet, Yifan Shi, Shefali Patel and Brian Geist. Analysis and interpretation of data: all authors; funding acquisition: Beverly Knight; project administration, resources, software and supervision: Beverly Knight.

Funding. These studies were supported by Johnson & Johnson. Journal's Rapid Service Fee was funded by Johnson & Johnson.

Data Sharing Statement. The Johnson & Johnson data sharing policy is available at https://www.janssen.com/clinical-trials/transparency. As data are not publicly available, requests can be sent to the corresponding author.

Data Availability. The datasets generated and/or analyzed during the current study are available from the corresponding author on reasonable request.

Declarations

Conflict of Interest. Beverly Knight, Brinda Tammara, Shannon Dallas, Saro Mardirosian, Jianyao Wang, Aline Laenen, Laurent Leclercq, Karen DiLoreto, Lieve Adriaenssen, Darren Moss, David Polidori, Siladitya Ray Chaudhuri, Seonghee Park, Carlo Sensenhauser, Anthony Ndifor, Siddharth Sukumaran, Tristan Baguet, Yifan Shi, Shefali Patel, Brian Geist, Stephanie A Barros, Mario Monshouwer: Employee: Johnson & Johnson; Shareholder: may own stock/stock options in Johnson & Johnson. Nishit B Modi: Employee: Protagonist Therapeutics, Inc. Anne Fourie, Raymond Patch: Former employee: Johnson & Johnson; Shareholder: may own stock/stock options in Johnson & Johnson. Chengzao Sun, Sandeep Somani: Employee: Pinnacle

Medicines; Former employee: Johnson & Johnson; Shareholder: may own stock/stock options in Johnson & Johnson. Beverly Knight, Nishit B Modi, David Polidori and Anne Fourie are listed as inventors on United States patent application published as US20240254180, related to this work. Chengzao Sun, Sandeep Somani and Raymond Patch are listed as inventors on Patent Cooperation Treaty (PCT) international patent application published as WO2021/146441, related to this work.

Ethical Approval. Rat study protocols and procedures were conducted under the United Kingdom Home Office project license number PP9376768 that controls scientific procedures on animals in the United Kingdom under the Animals (Scientific Procedures) Act 1986. The regulations conform to the European Convention for the Protection of Vertebrate Animals Used for Experimental and Other Scientific Purposes (Strasbourg, Council of Europe) and achieve the standard of care required by the United States Department of Health and Human Services' Guide for the Care and Use of Laboratory Animals. Monkey study protocols and procedures were reviewed and approved by the Charles River (Nevada) Institutional Animal Care and Use Committee and were conducted in compliance with applicable sections of the Final Rules of the Animal Welfare Act regulations (Code of Federal Regulations, Title 9), the Public Health Service Policy on Humane Care and Use of Laboratory Animals from the Office of Laboratory Animal Welfare, the Guide for the Care and Use of Laboratory Animals from the National Research Council. The FIH study protocol was reviewed and approved by Alfred Hospital Ethics Committee (Project 613/20 HREC/69080/Alfred-2020). The Human Research Ethics Committee (HREC) gave written approval for the Phase 1 FIH study, in accordance with local regulations. The HREC was appropriately constituted and operated in accordance with the Notes for Guidance on Good Clinical Practice (GCP, CPMP/ICH/15/95), as adopted by the Australian Therapeutic Goods Administration (TGA, 2000) and the National Health and Medical Research Council (NHMRC) National Statement on Ethical Conduct in Human Research (2007, updated 2018). Each subject gave informed consent at the screening visit to participate in the study and publication. This study was conducted in accordance with the principles of the current Declaration of Helsinki (Ethical Principles for Medical Research Involving Human Subjects), the NHMRC National Statement on Ethical Conduct in Human Research (2007, updated 2018), and Notes for Guidance on GCP (CPMP/ICH/135/95) established from the International Conference on Harmonization guidelines and adopted by the Australian TGA (2000). All study investigations were undertaken by scientifically and medically qualified persons. The relative bioavailability study protocol was reviewed and approved by FAGG (federal agency for medicines and health products in Belgium; reference number R&D/1317536). The study was conducted in accordance with the ethical principles that have their origin in the Declaration of Helsinki and that are consistent with GCPs and applicable regulatory requirements. Informed consent was gained prior to the commencement of any study procedures.

REFERENCES

1. Krueger JG, Eyerich K, Kuchroo VK, et al. IL-23 past, present, and future: a roadmap to advancing IL-23 science and therapy. Front Immunol. 2024;15:1331217.

2. Yang K, Oak ASW, Elewski BE. Use of IL-23 inhibitors for the treatment of plaque psoriasis and psoriatic arthritis: a comprehensive review. Am J Clin Dermatol. 2021;22:173–92.

3. Fanizza J, D'Amico F, Lusetti F, et al. The role of IL-23 inhibitors in Crohn's disease. J Clin Med. 2023;13:224.

4. Drakos A, Torres T, Vender R. Emerging oral therapies for the treatment of psoriasis: a review of pipeline agents. Pharmaceutics. 2024;16:111.

5. Feldman SR, Holmen Moeller A, Erntoft Idemyr ST, Gonzalez JM. Relative importance of mode of administration in treatment preferences among plaque psoriasis patients in the United States. J Health Econ Outcomes Res. 2017;4:141–57.

6. McLenon J, Rogers MAM. The fear of needles: a systematic review and meta-analysis. J Adv Nurs. 2019;75:30–42.

7. Armstrong AW, Puig L, Joshi A, et al. Comparison of biologics and oral treatments for plaque psoriasis: a meta-analysis. JAMA Dermatol. 2020;156:258–69.

8. Armstrong AW, Gooderham M, Warren RB, et al. Deucravacitinib versus placebo and apremilast in moderate to severe plaque psoriasis: efficacy and safety results from the 52-week, randomized, double-blinded, placebo-controlled phase 3 POETYK PSO-1 trial. J Am Acad Dermatol. 2023;88:29–39.

9. Strober B, Thaci D, Sofen H, et al. Deucravacitinib versus placebo and apremilast in moderate to severe plaque psoriasis: efficacy and safety results from the 52-week, randomized, double-blinded, phase 3 Program fOr Evaluation of TYK2 inhibitor psoriasis second trial. J Am Acad Dermatol. 2023;88:40–51.

10. Vinogradov AA, Yin Y, Suga H. Macrocyclic peptides as drug candidates: recent progress and remaining challenges. J Am Chem Soc. 2019;141:4167–81.

11. Nielsen DS, Shepherd NE, Xu W, et al. Orally absorbed cyclic peptides. Chem Rev. 2017;117:8094–128.

12. Fourie AM, Cheng X, Chang L, et al. JNJ-77242113, a highly potent, selective peptide targeting the IL-23 receptor, provides robust IL-23 pathway inhibition upon oral dosing in rats and humans. Sci Rep. 2024;14:17515.

13. Bissonnette R, Pinter A, Ferris LK, et al. An oral interleukin-23-receptor antagonist peptide for plaque psoriasis. N Engl J Med. 2024;390:510–21.

14. Ferris LK, Bagel J, Huang YH, et al. FRONTIER-2: a phase 2b, long-term extension, dose-ranging study of oral JNJ-77242113 for the treatment of moderate-to-severe plaque psoriasis. J Am Acad Dermatol. 2024;92:495–502.

15. Van de Graaff KM. Anatomy and physiology of the gastrointestinal tract. Pediatr Infect Dis. 1986;5:S11–6.

16. Mahato RI, Narang AS, Thoma L, Miller DD. Emerging trends in oral delivery of peptide and protein drugs. Crit Rev Ther Drug Carrier Syst. 2003;20:153–214.

17. Lipinski CA. Rule of five in 2015 and beyond: target and ligand structural limitations, ligand chemistry structure and drug discovery project decisions. Adv Drug Deliv Rev. 2016;101:34–41.

18. Sall C, Argikar U, Fonseca K, et al. Industry perspective on therapeutic peptide drug-drug interaction assessments during drug development: a European Federation of Pharmaceutical Industries and Associations white paper. Clin Pharmacol Ther. 2023;113:1199–216.

19. Drucker DJ. Advances in oral peptide therapeutics. Nat Rev Drug Discov. 2020;19:277–89.

20. Shah DK, Betts AM. Antibody biodistribution coefficients: inferring tissue concentrations of monoclonal antibodies based on the plasma concentrations in several preclinical species and human. MAbs. 2013;5:297–305.

21. Dragatin C, Polus F, Bodenlenz M, et al. Secukinumab distributes into dermal interstitial fluid of psoriasis patients as demonstrated by open flow microperfusion. Exp Dermatol. 2016;25:157–9.

22. Di L. Strategic approaches to optimizing peptide ADME properties. AAPS J. 2015;17:134–43.

23. Diao L, Meibohm B. Pharmacokinetics and pharmacokinetic-pharmacodynamic correlations of therapeutic peptides. Clin Pharmacokinet. 2013;52:855–68.

24. Papp KA, Langley RG, Lebwohl M, et al. Efficacy and safety of ustekinumab, a human interleukin-12/23 monoclonal antibody, in patients with psoriasis: 52-week results from a randomised,

double-blind, placebo-controlled trial (PHOENIX 2). Lancet. 2008;371:1675–84.

25. Reich K, Armstrong AW, Foley P, et al. Efficacy and safety of guselkumab, an anti-interleukin-23 monoclonal antibody, compared with adalimumab for the treatment of patients with moderate to severe psoriasis with randomized withdrawal and retreatment: Results from the phase III, double-blind, placebo- and active comparator-controlled VOYAGE 2 trial. J Am Acad Dermatol. 2017;76:418–31.

26. Reich K, Gooderham M, Thaci D, et al. Risankizumab compared with adalimumab in patients with moderate-to-severe plaque psoriasis (IMMvent): a randomised, double-blind, active-comparator-controlled phase 3 trial. Lancet. 2019;394:576–86.

27. Reich K, Papp KA, Blauvelt A, et al. Tildrakizumab versus placebo or etanercept for chronic plaque psoriasis (reSURFACE 1 and reSURFACE 2): results from two randomised controlled, phase 3 trials. Lancet. 2017;390:276–88.